# Incorporating DEADBEAT and Low Frequency Harmonic Elimination in Modular Multilevel Converters (MMC)


| | |
|---|---|
| Journal: | *IET Generation, Transmission & Distribution* |
| Manuscript ID: | GTD-2014-0429 |
| Manuscript Type: | Research Paper |
| Date Submitted by the Author: | 08-May-2014 |
| Complete List of Authors: | Wang, Can; McGill University, Electrical & Computer Engineering<br>Ooi, Boon-Teck; McGill University, Electrical and Computer Engineering |
| Keyword: | POWER ENGINEERING, POWER CONVERSION, POWER TRANSMISSION |
| | |

# Incorporating DEADBEAT and Low Frequency Harmonic Elimination in Modular Multilevel Converters (MMC)

Can Wang, and B. T. Ooi, *Life Fellow, IEEE*

Can Wang is now with Department of Electrical and Computer Engineering, McGill University, Montreal, H3A 0E9, QC, Canada (email: can.wang@mail.mcgill.ca)

Boon-Teck Ooi is now with Department of Electrical and Computer Engineering, McGill University, Montreal, H3A 0E9, QC, Canada (email: boon-teck.ooi@mcgill.ca)

***Abstract*— The paper shows that MMC can implement deadbeat control and harmonic elimination together. MMC, under deadbeat control, tracks the current reference exclusively, so that it is: (i) safe from large destructive currents of ac faults; (ii) free from the odd harmonics generated by the nonlinearities of MMC. As deadbeat control cannot filter even harmonics on the dc side, harmonic elimination has to be done by joint feedback-feedforward methods. However, the cost saving from capacitor size reduction, made possible by the harmonic elimination, comes to naught when large ac fault currents charge the capacitors to voltage levels destructive to IGBTs. Deadbeat, in preventing the flow of large fault currents, safeguards capacitor size reduction made possible by the harmonic elimination methods. Redundant protection by the methods enhances reliability. Claims are validated by simulations by SIMULINK of MATLAB.**

***Index Terms*: modular multilevel converter (MMC), dead-beat, reference current control, feedforward, feedback, harmonic function analysis, Fliege notch filter, complement notch filter**

## 1. Introduction

The innovative modular multilevel converter topology has spawned research in many directions: (i) applications to High Voltage DC Transmission (HVDC) [1]-[8], Flexible AC Transmission Systems (FACTS) [9]-[11], medium voltage motor drives [12]-[14]; (ii) fundamental understanding of the topology through mathematical modeling and harmonic function analysis [15]-[23]; (iii) finding improvements in novel techniques in modulation [24]-[26] and harmonics reduction [27]-[32].

Reference Current Control is important in protecting converters from ac faults. When ac currents are regulated at reference values, they are prevented from growing to destructive levels during faults. Using deadbeat control to make Voltage Source Converters (VSCs) operate under Reference Current Control is a frequent practice [33]-[40]. Under deadbeat, the VSCs have fast response, delay of 2 computation steps for example. Deadbeat in VSCs prevents harmonics from the dc side from crossing over to the ac-side [39]. Deadbeat, in enforcing reference signal tracking, should stop 3rd and odd harmonics generated by nonlinearities of MMC from emerging on the ac currents. But does MMC accept deadbeat control? This paper answers in the affirmative. However as [41] shows, research on deadbeat for MMC has only just begun.

Because the even harmonics in the circulating current are on the dc side, deadbeat cannot eliminate them. Therefore, in order to reduce the size and cost of large sub-module capacitors which are required to filter the even harmonics, the feedback methods of [27]-[32] and the feedforward method in [23] have to be used. These harmonic elimination methods come to naught, if during faults the ac fault currents charge the capacitors of reduced size, so that their dc voltages rise above the safe voltage limit of IGBTs. Deadbeat rescues the elimination methods by preventing large fault currents. But can MMC implement both deadbeat and harmonic elimination together?

The joint implementation of deadbeat and harmonic elimination methods by MMC is possible by following the results of harmonic function analysis of [23], which has shown that MMC has two decoupled amplification channels: (i) a fundamental frequency channel of the modulation signal to produce an amplified voltage of $U_{ref}\cos(\omega t+\delta)$ on the ac-side; (ii) a 2nd harmonic channel of the modulation signal '$Y\cos(2\omega t+\gamma)$' which produces an amplified voltage on the dc side. Deadbeat is implemented in the fundamental frequency channel and harmonic elimination in the 2nd harmonic channel of $Y\cos(2\omega t+\gamma)$. As the theoretical base of this paper depends on Table 1 to 4 of [23], the tables are reproduced in Appendix 1 for easy reference.

The objectives of this paper are to show how, (i) deadbeat, in open loop and with closed loop current feedback, (ii) feedforward and feedback to eliminate low frequency harmonics, can be implemented by MMC.

The multiple objectives are fulfilled as follows: Section 2 briefly reviews the derivation of Table 1 to 4 of [23]. Section 3 presents the principles deadbeat. Section 4 presents simulation results of successful deadbeat implementation. Section 5 reviews the feedforward method of [23] and presents a feedback method based on the innovative Complement Notch Filter to identify the 2nd harmonic as the "error" for negative feedback elimination. Section 6 presents simulations of joint application of deadbeat, feedback and feedforward harmonic elimination. Conclusions are presented in Section 7.

## 2. Modular Multilevel Converter (MMC) Topology and Control

The objective of this section is to show that MMC has one channel to implement deadbeat and another channel to implement harmonic elimination. The two independent channels are found in the formulas of Tables 1 to 4 in [23]. In order to have confidence in the formulas, a brief review is given on how they have been derived. This section also introduces the model of the 3-phase MMC, as shown in Fig. 1, because performance claims are validated by simulations (SIMULINK of MATLAB) of the software model of Fig.1.

The operation of MMC (schematic shown in Fig. 1(a)) is based on applying modulation signal $m_U(t)$ to the upper arm and $m_L(t)$ to the lower arm of each phase in the forms of:

$$m_U(t) = \frac{1}{2} - \frac{U_{ref}}{U_{dc}}\cos(\omega t + \delta) \tag{1-a}$$

$$m_L(t) = \frac{1}{2} + \frac{U_{ref}}{U_{dc}}\cos(\omega t + \delta) \tag{1-b}$$

The IGBTs of the sub-modules (see insets in Fig. 1 (a) and (b)) connect $n_U(t)$ and $n_L(t)$ capacitors which are proportional to the modulation signals:

$$n_U(t) = N[\frac{1}{2} - \frac{U_{ref}}{U_{dc}}\cos(\omega t + \delta)] \tag{2-a}$$

$$n_L(t) = N[\frac{1}{2} + \frac{U_{ref}}{U_{dc}}\cos(\omega t + \delta)] \tag{2-b}$$

As illustrated in Fig. 1(b), the IGBTs in each sub-module either bypass its capacitor or connect its capacitor to form a series string.

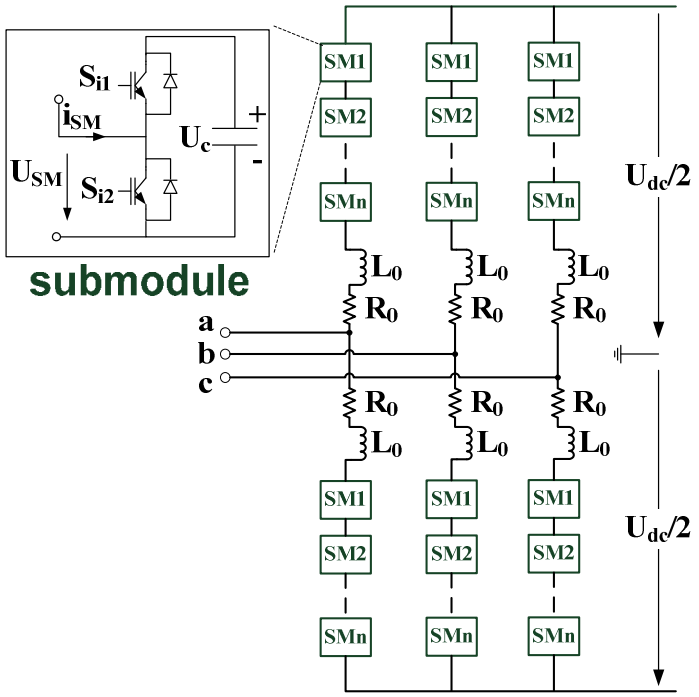


Fig. 1 (a) Schematic of 3-phase MMC Station consisting of connections of sub-modules shown by inset.

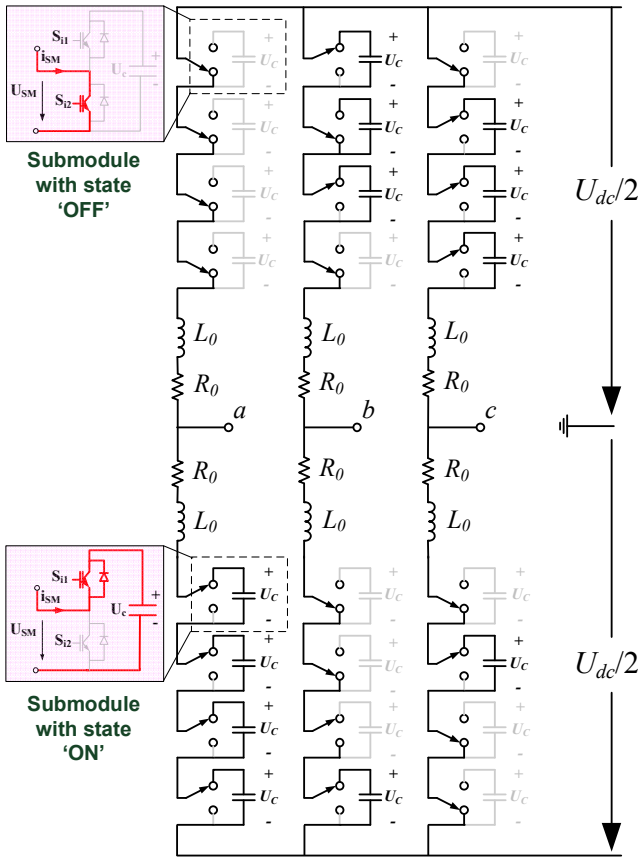


Fig. 1 (b) Illustration of the operation based on IGBTs of sub-modules bypassing capacitors or connecting capacitors in series to form a string.

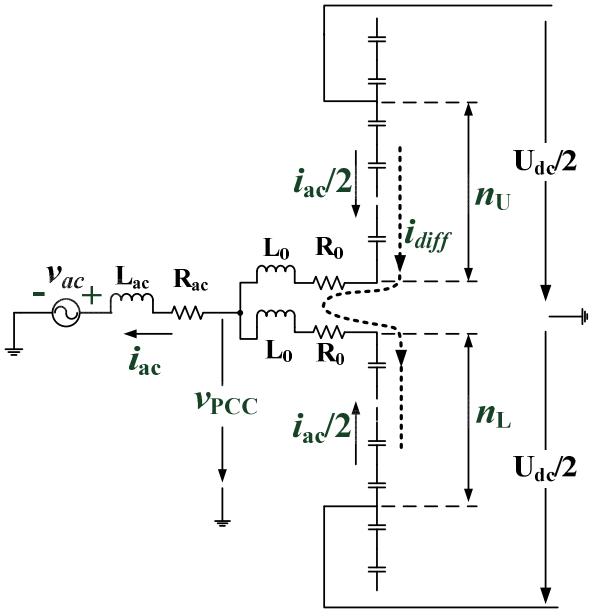


Fig. 2 One phase of MMC showing $n_U$ capacitor string in upper arm and $n_L$ capacitor string in lower arm.

*Upper Arm*

Fig. 2 shows the strings of capacitor of one phase. Consider the upper arm of Fig. 2 only. For a string of $n_U(t)$ capacitors, each of size $C$, the equivalent capacitor is $C/n_U(t)$. The voltage $u(t)$ across *a single* capacitor charged by current $n_U(t)(0.5i_{ac}+i_{diff})$, shown in Fig.2, is:

$$C\frac{du}{dt} = n_U(t)(0.5i_{ac} + i_{diff}) \tag{3}$$

Multiplying (3) by the modulation signal $m_U(t)$ of (1-a), (3) becomes:

$$\frac{C}{N}\frac{du_U}{dt} = m_U(t)(0.5i_{ac} + i_{diff}) \tag{4}$$

where $u_U(t)$ is the voltage across equivalent capacitor of constant size $C/N$.

The ac current takes the form

$$i_{ac} = I_{ac}\cos(\omega t + \varphi_{ac}) \tag{5}$$

It is assumed that the current $i_{diff}$ consists of a dc current $I_d$ and an algebraic unknown 2nd harmonic current:

$$i_{diff} = I_d + i_{2\omega} \tag{6}$$

$$i_{2\omega} = X\cos(2\omega t + \varphi_2) \tag{7}$$

Because the 2nd harmonic current is the "medium" of harmonic proliferation, its amplitude is assigned the symbol "X" in (7) so that its spread in Tables 1 and 2 is readily identified.

Substitution (5), (6) and (7) in (4)

$$\frac{C}{N}\frac{du_U}{dt} = [\frac{1}{2} - \frac{U_{ref}}{U_{dc}}\cos(\omega t + \delta)] \cdot \{\frac{I_{ac}}{2}\cos(\omega t + \varphi_{ac}) + [I_d + X\cos(2\omega t + \varphi_2)]\} \tag{8}$$

For bookkeeping convenience, the voltage $u_U$ is decomposed as:

$$u_U = 2T_1 + 2T_2 + 2T_3 + 2T_4 \tag{9}$$

The integration of the 4 components of (9) in (8) yields:

$$\frac{d2T_1}{dt} = \frac{N}{C}[\frac{I_{ac}}{4}\cos(\omega t + \varphi_{ac})] \tag{10}$$

$$\frac{d2T_2}{dt} = \frac{N}{C}[\frac{I_d}{2} - \frac{U_{ref}}{4U_{dc}}\cos(\delta - \varphi_{ac})] \tag{11}$$

$$\frac{d2T_3}{dt} = \frac{N}{C}[\frac{X\cos(2\omega t + \varphi_2)}{2} - \frac{U_{ref}I_{ac}}{4U_{dc}}\cos(2\omega t + \varphi_{ac} + \delta)] \tag{12}$$

$$\frac{d2T_4}{dt} = \frac{N}{C}\{[I_d + X\cos(2\omega t + \varphi_2)] \cdot [\frac{U_{ref}}{U_{dc}}\cos(\omega t + \delta)]\} \tag{13}$$

On integration, the voltage terms $T_1$, $T_2$, $T_3$ *and* $T_4$ are listed in Tables 1 and 2 in Appendix 1.

For modulation signal of (1-a), $n_U$ capacitors of (2-a) are connected in series as illustrated in Fig. 2. Therefore, the voltage $u_{upper}$ across $n_U$ capacitors is

$$\begin{aligned} u_{upper} &= n_U \frac{u_U}{N} \\ &= [\frac{1}{2} - \frac{U_{ref}}{U_{dc}}\cos(\omega t + \delta)] \cdot 2(T_1 + T_2 + T_3 + \mathrm{T}_4) \\ &= T_1 + T_2 + T_3 + \mathrm{T}_4 + T_5 + T_6 + T_7 + \mathrm{T}_8 \end{aligned} \tag{14}$$

where the formulas of $T_5$, $T_6$, $T_7$ and $T_8$ are

$$T_{m+4} = -\frac{U_{ref}}{U_{dc}}\cos(\omega t + \delta) \cdot 2T_m \qquad \text{for } m=1,2,3,4 \tag{15}$$

$T_5$, $T_6$, $T_7$ and $T_8$ are also in Table 1 and 2.

*Lower Arm*

Following the same development, the voltage across the terminals of the lower arm is:

$$u_{lower} = -T_1 + T_2 + T_3 - T_4 + T_5 - T_6 - T_7 + T_8 \tag{16}$$

*Equivalent Circuit of Single Phase*

By combining the Upper Arm and Lower Arm, [23] shows that an MMC arm is modeled by ideal voltage sources shown in Fig. 3(a) on the ac-side and Fig. 3(b) on the dc side.

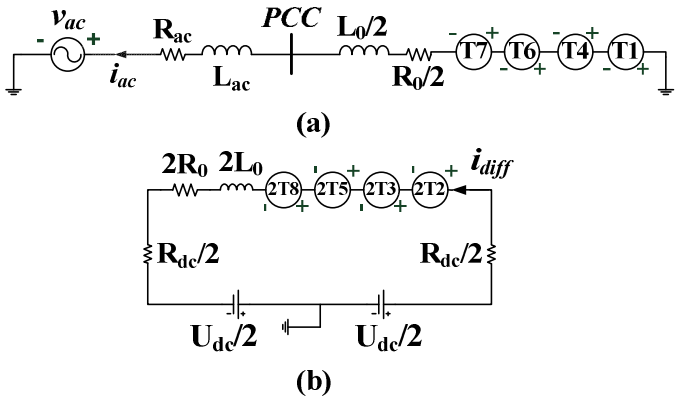


Fig. 3 MMC phase represented by ideal voltages: (a) ac-side; (b) dc-side.

*Fundamental Frequency Channel of* $U_{ref}\cos(\omega t+\delta)$

Referring to Fig. 3(b) and Table 2, on the dc side the significant voltage is $T_2$.

$$T_2=\frac{N}{2C}\int_{-\infty}^{t}[\frac{I_d}{2}-\frac{U_{ref}I_{ac}}{4U_{DC}}\cos(\delta-\varphi_{ac})]d\tau \tag{17}$$

$T_2$ is the voltage of ac-to-dc power balance. In steady-state power balance, $2T_2=U_{dc}$.

Referring to Fig. 3(a) and Table 1, the significant voltage on the ac side is $T_6$

$$\begin{aligned}T_6&=-\frac{NU_{ref}}{CU_{dc}}\cos(\omega t+\delta)\cdot\int_{-\infty}^{t}[\frac{I_d}{2}-\frac{U_{ref}I_{ac}}{4U_{DC}}\cos(\delta-\varphi_{ac})]d\tau\\&=-\frac{U_{ref}}{U_{dc}}\cos(\omega t+\delta).2T_2=-U_{ref}\cos(\omega t+\delta)\end{aligned} \tag{18}$$

From (18), one concludes that the sinusoidal component of the modulation signal $(U_{ref}/U_{dc})\cos(\omega t+\delta)$ has $T_6$ as its amplified voltage on the ac-side.

*Channel for 2nd Harmonic Modulation Signal* $Y\cos(2\omega t+\gamma)$

Ref. [23] considers adding $u_{add}=Y\cos(2\omega t+\gamma)$ to the modulation signal to (1-a) and (1-b) so that they take the forms of:

$$m_U(t)=\frac{1}{2}-\frac{U_{ref}}{U_{dc}}\cos(\omega t+\delta)+\frac{Y}{U_{dc}}\cos(2\omega t+\gamma) \tag{19-a}$$

$$m_L(t)=\frac{1}{2}+\frac{U_{ref}}{U_{dc}}\cos(\omega t+\delta)+\frac{Y}{U_{dc}}\cos(2\omega t+\gamma) \tag{19-b}$$

Table 3 and Table 4 are obtained by following the same procedure in deriving Table 1 and Table 2. To simplify bookkeeping, it is assumed that the second harmonic currents bearing "X" have already been eliminated. In order that the effect of $u_{add}$ stands out, "$Y$" is given as its amplitude. There are entries bearing "$Y$" everywhere in Tables 3 and 4. The terms bearing "Y" are numerically small compared to $T_F$.

$$T_F = Y\cos(2\omega t + \gamma) \tag{20}$$

$T_F$, on the dc side, is the amplified voltage of the 2nd harmonic modulation signal in (19). Therefore MMC has an independent channel whereby $T_F$ is applied through feedforward and or feedback to counteract the source 2nd harmonic voltages in Table 2.

## 3. Deadbeat Control

Most texts on deadbeat make use of sampled data formulations and z-transforms. For readers, who are more familiar with time-domain, this section presents the principles of deadbeat from linear system theory where the transfer function H(s) is the Laplace Transform of the impulse response. A distinctive feature of the deadbeat control in this paper is that it does not require d-q transformation. As an individual phase controller, it handles asymmetric operating conditions, such as a single-line fault. [Notations used in this section: $u_{-1}(t)$, $u_0(t)$ are symbols of step, impulse function. $du_{-1}(t)/dt=u_0(t)$]

### *3-A Open Loop Deadbeat*

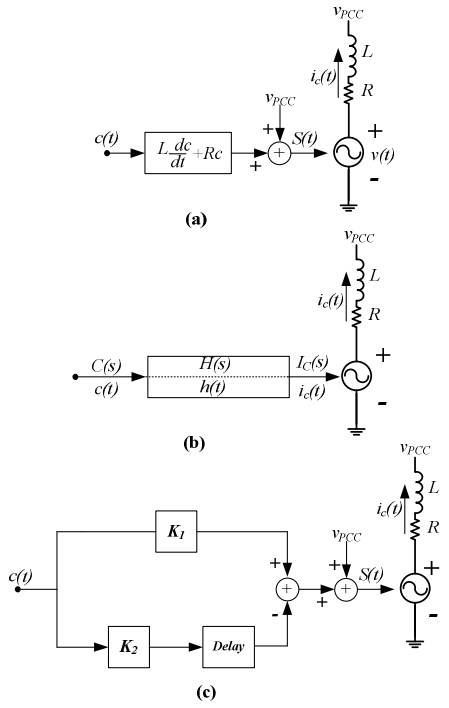


Fig. 4 Reference Current Control: (a) Ideal implementation; (b) Transfer Function of Implementation; (c) Deadbeat Implementation.

Fig. 4 is used to present the principles of deadbeat in time domain. "Plant", in deadbeat terminology, consists of "*L*" and "*R*" in Fig. 4. Referring to Fig. 2 and Fig. 3(a), $L=L_0/2$, $R=R_0/2$. In Fig. 4 (a), the "plant" lies between

$v_{PCC}(t)$, the voltage of the point of common coupling (PCC), and $v(t)=T_6$, the voltage produced by $U_{ref}\cos(\omega t+\delta)$ channel. The current $i_C(t)$ in the "plant" is $i_{ac}(t)$.

*3-A-1 Reference Current Control*

In *Reference Current Control*, an ideal voltage-source $v(t)$ is required that to produce a current $i_C(t)$ in response to reference current command $c(t)$. In Fig. 4(a), from Kirchhoff's Voltage Law, the current $i_C(t)$ is solved from

$$L\frac{di_C}{dt}(t)+Ri_C(t)=v(t)-v_{PCC}(t) \tag{21}$$

On the ac-side of the MMC, $v_{PCC}(t)$, the voltage measured at the PCC, is a sinusoidal voltage at line frequency. When the reference current $c(t)$ is also a line frequency sinusoidal signal, the sinusoidal component of the modulation signal $S(t)$ is also line frequency sinusoidal term. Writing

$$S(t)=\frac{1}{A}\left[L\frac{dc(t)}{dt}+Rc(t)+v_{PCC}(t)\right] \tag{22}$$

where $A$ is the amplification gain and substituting $v(t)=AS(t)$ in (21)

$$L\frac{di_C(t)}{dt}+Ri_C(t)=L\frac{dc(t)}{dt}+Rc(t) \tag{23}$$

The equality in (23) means that the plant current $i_C(t)$ tracks the current reference signal $c(t)$, that is

$$i_C(t)=c(t) \tag{24}$$

Because $Ldc(t)/dt$ cannot be implemented accurately, the deadbeat method serves as a good approximation.

*3-A-2 Transfer Function Approach*

Taking the Laplace Transform by which $i_C(t)\rightarrow I_C(s)$, $c(t)\rightarrow C(s)$, (24) is expressed by the transfer function relationship as:

$$I_C(\mathrm{s})=H(s)C(s) \quad \text{where } H(s)=1 \quad \text{for } -\mathrm{j}\infty\le S\le+\mathrm{j}\infty \tag{25}$$

The time domain equivalent of (25) is the convolution integral relationship

$$i_C(t)=\int_{-\infty}^{t}c(\tau)h(t-\tau)d\tau \tag{26}$$

where $h(t-\tau)$ is the impulse response of $H(s)$. For $H(s)=1$, the impulse response has to be the impulse function $u_0(t-\tau)$.

Fig. 4(b) shows the relationship of (25) and (26) in block diagram form. An impulse is a waveform with infinitesimally narrow width w and height 1/w so that the area of the pulse is 1. When $h(t-\tau)$ is the impulse function

$u_0(t\text{-}\tau)$ in (26), then $i_C(t)=c(t)$. This is because the impulse function $u_0(t\text{-}\tau)$ is zero everywhere from $\tau$= -∞ to $\tau=t$ so that the integral in (26) is zero everywhere except at $\tau=t$. At $\tau=t$, because $u_0(t\text{-}\tau)$ has unity area. When multiplied by c($\tau$), the integral yields $i_C(t)=c(t)$.

The deadbeat method, as implemented by Fig. 4(c), is based on creating a very narrow current pulse whose area is unity and therefore approximates the impulse response of the transfer function $H(s)$=1.

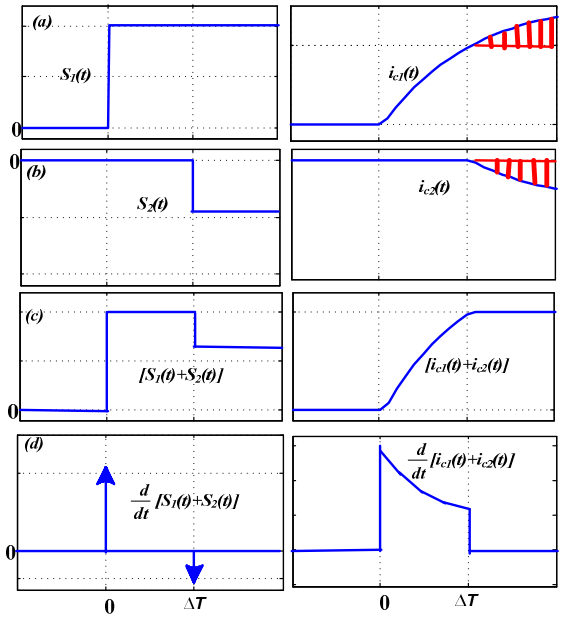


Fig. 5 Illustrations of construction of dead-beat block diagram. (*a*) step input $S_1(t)$; (*b*) delayed step input $S_2(t)$; (*c*) $S_1(t)+S_2(t)$; (*d*) $d[S_1(t)+S_2(t)]/dt$.(left) voltage waveforms; (right) response waveform of current in "*L-R* plant"

*3-A-3 Constructing Deadbeat Control Block*

The blocks in Fig. 4(c) preconditions the current reference $c(t)$ so that its output when added to feedforward voltage $v_{PPC}(t)$ becomes the modulation signal '$S(t)$'. As the voltage at the point of common coupling is equal and opposite to the feedforward component $v_{PPC}(t)$ in v(t), the gains $K_1$, $K_2$ and the delay are designed to ensure that for input as an impulse current reference $c(0)=u_0(0)$, the voltage-source $v(t)$ outputs current which is a close approximation of $i_C$(t)= $u_0(0)$.

The steps to the construction of the block of $K_1$, $K_2$ and the delay are illustrated in Fig. 5. The graph on the left of Fig. 5(a) illustrates a step input to the modulation signal, $S_1u_{-1}(0)$. In response to the step voltage

$$v(t) = AS_1u_{-1}(0) \tag{27}$$

From $T_6$ of (18), the amplification gain $A=U_{dc}$ and the well-known solution of the differential equation (23), the current to the step voltage is

$$i_{C1}(t) = U_{dc}\frac{S_1}{R}(1-e^{-\frac{R}{L}t}) \tag{28}$$

The long time response of the current, illustrated on the graph on the right, is reduced by adding a time-delayed negative step input $S_2u_{-1}(-\Delta T)$ (magnitude $S_2$ after delay of $\Delta T$) as illustrated in the left of Fig. 5(b). Its current response is shown on the right of Fig. 5(b).

Using the formula of (28) to scale $S_2$ with respect to $S_1$ and $\Delta T$ so that the shaded portion of the current in (b) cancels that of (a), the slow response is lopped off as shown on the right of Fig. 5(c). The modulation signal which produces the current is $S_1u_{-1}(0)+S_2u_{-1}(-\Delta T)$, the sum of the inputs of Fig. 5(a) and (b) as illustrated on the left of Fig. 5(c).

From system theory, an impulse function is obtained by differentiating a step function. The left of Fig. 5(d) illustrates the two impulses obtained by differentiating the step functions in the left of Fig. 5(c). Also, the current output in Fig. 5(d) is the differentiated form of the current on the right of Fig. 5(c). On differentiating (28)

$$\frac{di_C(t)}{dt} = U_{dc}\frac{S_1}{L}e^{-\frac{R}{L}t} \qquad 0 \le t \le \Delta T \tag{29}$$

For small $\Delta T$, the narrow pulse has an approximate area of $\Delta TU_{dc}S_1/L$ which has the dimension of the current. The narrow pulse of Fig. 5(d) can be approximated as an impulse. Since the area is the gain, it follows that

$$\left|H(j\omega)\right| = U_{dc}S_1\frac{\Delta T}{L} \tag{30}$$

The block diagram of Fig. 4(c) is developed from Fig. 5. The formulas of $K_1$ and $K_2$ are derived as:

$$K_1 = \frac{L}{\Delta T} \tag{31}$$

$$K_2 = \frac{L}{\Delta T} - R \tag{32}$$

The "delay" block contains $\Delta T$. Since $c(t)$ and $v_{PCC}(t)$ are fundamental frequency waveforms, $S(t)$ has the functional form of $U_{ref}\cos(\omega t + \delta)$ in (1). The MMC produces this voltage as $T_6$.

*3-B Close-Loop Deadbeat*

MMC has to operate in the face of uncertainties. The voltages $v_{PCC\text{-}a}(t)$, $v_{PCC\text{-}b}(t)$ and $v_{PCC\text{-}c}(t)$ at the points of common coupling immunize, to some extent, the uncertainties in the ac-circuits outside the MMC. Because the components L and R belong to the manufacturer and can be measured precisely, deadbeat can be designed with confidence. But parameters change with temperature and other climatic factors. Close-loop feedback control, in

general, makes performance insensitive to parameter variations. Closed loop feedback control is implemented as shown in Fig. 6 [40].

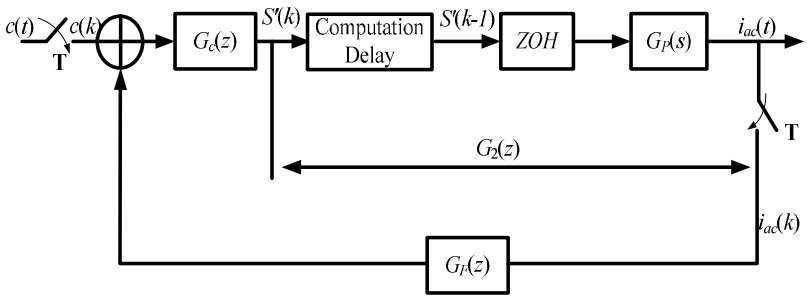


Fig. 6.Schematic of local current feedback of deadbeat

Because of a delay block has to be represented by exponential transfer function $e^{-a\Delta T}$, analysis is easier by passing from the "s-domain" to the "z-domain" of sampled data analysis. In the feedback block diagram shown in Fig. 6, the implementation of sampling is illustrated by the opening and closing of switches "*T*" so that $c(t)$ becomes $c(k)$. The objective is to design the closed loop deadbeat to have delay of $2\Delta T$. The overall transfer function is $z^{-2}$.

In Fig. 6, its output $S'(k)$ in Fig. 6, is added to $v_{PCC}(t)$. Their sum becomes the sinusoidal component of the modulation signal $S(t)$ in Fig. 4(c).

In continuous time domain, the Zero-Order-Hold block and the plant (L-R) in Fig. 4 are:

$$G_{ZOH}(s) = \frac{1-e^{-s\Delta T}}{s} \tag{33}$$

$$G_P(s) = \frac{b}{s+a} \tag{34}$$

Here, $a=R/L$, $b=1/L$. Taking the Z transform of $G_{ZOH}(s)G_P(s)$,

$$G_{ZOH}G_P(z) = \frac{a}{b}\frac{1-e^{-a\Delta T}}{1-e^{-a\Delta T}z^{-1}}z^{-1} \tag{35}$$

Including the computational delay of $z^{-1}$ in Fig. 6, the overall transfer function is designed to be:

$$G(z) = \frac{G_C(z)z^{-1}G_{ZOH}G_P(z)}{1+G_F(z)G_C(z)z^{-1}G_{ZOH}G_P(z)} = z^{-2} \tag{36}$$

which has a sampling delay of two sampling periods. The controller blocks $G_C(z)$ and $G_F(z)$ can be derived as:

$$G_C(z) = \frac{a}{b}\frac{1}{1-e^{-a\Delta T}}\frac{1}{1+e^{-a\Delta T}z^{-1}} \tag{37}$$

$$G_F(z) = e^{-2a\Delta T} \tag{38}$$

Detail derivation of closed loop blocks is given in [40].

## 4. Simulation Tests on MMC under Deadbeat Control

Simulation software has been developed for the 3-phase MMC station of Fig.1. Table 5 in Appendix 2 lists the parameters used for the 12-level model of the MMC station. The simulation software goes to the detail of "Phase-shifted triangle carrier Sinusoidal pulse Width Modulation (SPWM)" and the sorting algorithm, taken from [42], to ensure that the voltages of the capacitors of each string are balanced. Ref. [43] presents other methods of balancing. Extensive validation tests in [23] show that time-series simulations agree with predictions from harmonic functional analysis to the extent that their waveforms lie on top of each other.

*Test on Capability of Closed Loop Deadbeat to Eliminate Harmonics*

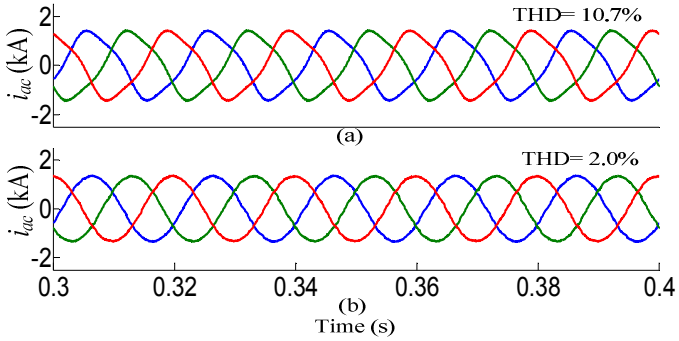


Fig. 7 Simulated 3-phase AC currents when ac-side transformers have grounded wye connection. (a) without deadbeat control; (b) under closed loop deadbeat control.

$T_4$ and $T_7$ in Table 1 of [23] have 3rd harmonic voltage components on the ac-side. Normally, the ac sides of MMC stations are connected to transformers in delta or open wye to exclude the 3rd harmonic current generated by $T_4$ *and* $T_7$. The simulation test consists of connecting the MMC to transformers in wye with the neutral grounded. As shown in Fig. 7(a), the 3-phase current waveforms have large 3rd harmonics, confirming the predictions of [23]. When the MMC station operates under deadbeat with current feedback as shown in Fig. 6, the 3rd harmonic is not noticeable in Fig. 7(b). This confirms experience with VSCs in [39]; closed loop deadbeat prevents harmonics from flowing to ac-side. The current THD is reduced from 10.7 % to 2%.

*Test on Capability of Deadbeat to Protect MMC against Ground Fault*

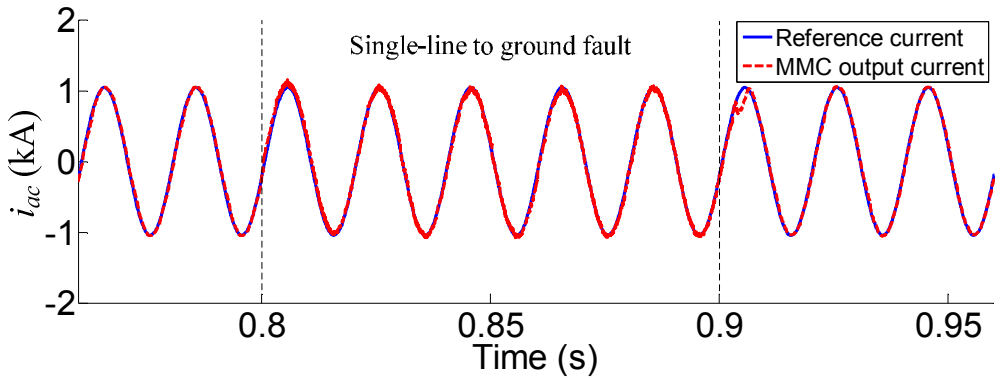


Fig. 8 AC current of one MMC phase tracking Current Reference during a single-line to ground fault 0.8$s$≤t≤0.9$s$. Deadbeat Control

Under deadbeat control, the ac phase current (red) tracks the Current Reference (blue) even when the severe single-line to ground fault occurs at PCC during 0.8$s$ ≤t ≤ 0.9$s$ as shown in Fig. 8. This is because the measured voltage at the point of common connection $v_{PCC}(t)$ is fedforward as shown in Fig. 4(a) and (c). As $v_{PCC}(t)$ drops to ground voltage, $v(t)$, which follows $(U_{ref}/U_{dc})\cos(\omega t+\delta)$) of $T_6$, also drops to a value just sufficient to drive $i_C(t)$ across $L$ and $R$.

5. Feedforward and Feedback Harmonic Elimination

Functional Analysis of [23] shows that the origin of low frequency harmonics comes from voltage components without "$X$" in $T_3$, $T_5$ and $T_8$ in the 2nd harmonic column of Table 2. Their voltages cause the flow of 2nd harmonic current $i_{2\omega} = X\cos(2\omega t + \varphi_2)$ of (7). The 2nd harmonic current then proliferates to other low frequency harmonic voltages in Tables 1 and 2, identified by "$X$". Therefore if a voltage can be introduced which cancels the source 2nd harmonic voltages, then not only is the 2nd harmonic eliminated but the other low harmonics proliferated by it as well.

*Feedforward Method*

The voltage components $T_{3\text{-}2\omega\text{-}ii}$, $T_{5\text{-}2\omega}$ and $T_{8\text{-}2\omega\text{-}i}$ in Table 2 are considered to be the original source of 2nd harmonic because they do not bear the "$X$" term. The 2nd harmonic current is eliminated at the source if the voltage $T_F$ controlled by $u_{add}(t)=Y\cos(2\omega t+\gamma)$ cancels the total source voltages:

$$\begin{aligned} T_F &= -[T_{3-2\omega-ii} + T_{5-2\omega} + T_{8-2\omega-i}] \\ &= -\frac{NU_{ref}^2 I_d}{2\omega C U_{dc}^2}\sin(2\omega t + 2\delta) + \frac{3NU_{ref} I_{ac}}{16\omega C U_{dc}}\sin(2\omega t + \delta + \varphi_{ac}) \end{aligned} \quad (39)$$

In [23], the authors have demonstrated the effectiveness of the feedforward elimination method for extensive ranges of operations.

*Feedback Method*

Feedback likewise makes use of $u_{add}(t)=Y\cos(2\omega t+\gamma)$. This signal is extracted from $i_{diff}$ of (6) shown in Fig. 2.

*Complement Notch Filter*

The authors propose an innovative Complement Notch Filter, shown in Fig. 9, to extract the 2nd harmonic from $i_{diff}$. Along the lower path of Fig. 9 (a), $i_{diff}$ passes that through the Fliege Notch Filter, tuned to the 2nd harmonic. Fig. 9 (b) and (c) respectively show the schematic of the Fliege Notch Filter [44] and its Bode diagram. The output of the lower path is subtracted from unfiltered $i_{diff}$ of the upper path. The result is a band pass filter centered at the 2nd harmonic whose Bode diagram is shown by Fig. 9 (d)---the complement of the "notch" of Fig. 9 (b). (Because it has better characteristics the Fliege Notch Filter has been chosen over the Twin-Tee Notch filter [44].)

The 2nd harmonic extract of $i_{diff}$ is subtracted from zero to become negative feedback error. The feedback error, after passing through a P-I block, is used as the modification component of the modulation signal , $u_{add}(t)=Y\cos(2\omega t+\gamma)$ in (19).

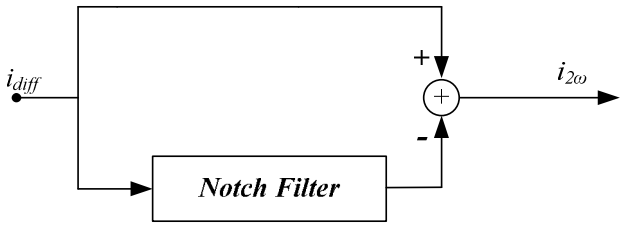


Fig. 9 (a) Complement Notch Filter

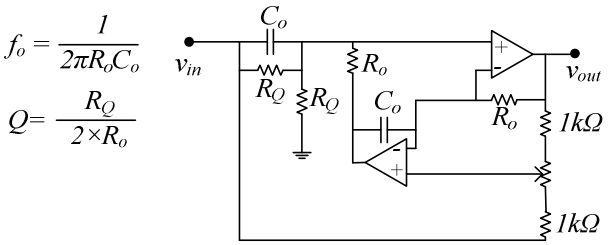


Fig. 9 (b) Fliege Notch Filter.

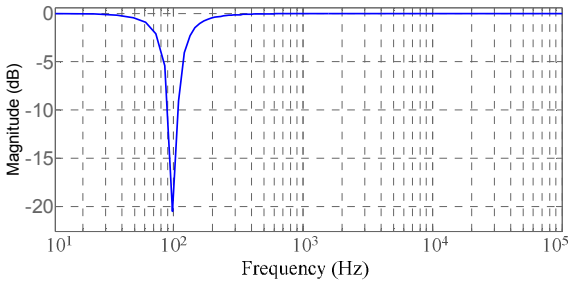

Fig. 9 (c) Magnitude-vs-frequency of Fliege Notch Filter

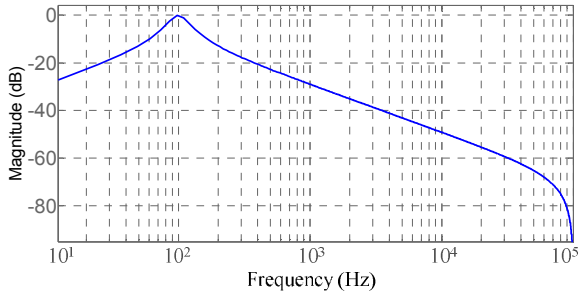


Fig. 9 (d) Magnitude-vs-frequency of Complement Notch Filter

## 6. Simulation Results on Harmonic Elimination and Deadbeat

*Robustness Test on Feedforward 2nd Harmonic Elimination*

Fig. 10 displays in (a) the 3-phase current, in (b) the second harmonic current $i_{2\omega}(t)$ of (7), in (c) $U_C(t)$, the capacitor voltage in each sub-module of phase A of the upper arm. Because deadbeat is not activated, the 3-phase ac currents reach very high values when a severe 3-phase line-to-ground fault at PCC is simulated between t=0.5s and t=0.6s. Although the 2nd and low frequency harmonics in (c) are reduced by feedforward elimination, the fault currents charge the capacitors to levels above the voltage rating of IGBTs.

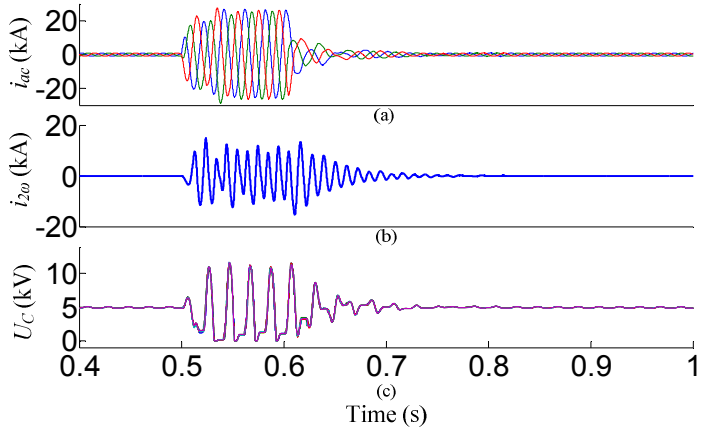


Fig. 10. (a) 3-phase ac current, (b) 2nd harmonic current component (c) voltages across capacitor (12 sub-modules superposed). Robustness test: 3-phase line-to-ground short circuit 0.5s ≤ t ≤ 0.6s. Feedforward elimination activated, Deadbeat not activated.

*Test on Capability of MMC to Implement Harmonic Elimination Methods and Deadbeat*

In this test, deadbeat control has been activated. Fig. 11 shows in (a) the 3-phase ac currents, (b) circulating current $i_{diff}$, (c) $U_C$, the voltage across one sub-module capacitor. In (c), the voltage $U_C$ fluctuates around the 5 kV average as the capacitor is charged by the 50 Hz of 0.5 $i_{ac}$ and the *2nd* and even harmonics of $i_{diff}$. At t=0.2s, feedforward, based on (39), is activated. The reduction of 2nd harmonic, associated with "*X*" in Table 2, is apparent

in (b) and (c). At t=0.5s, feedback using Complement Notch Filter of Fig. 9 is also activated. The 2nd harmonic in $i_{diff}$ is reduced further. Feedforward contributes by first reducing the size of the "error" before extraction by the Complement Notch Filter by the feedback stage. Thus the gain of the negative feedback stage does not have to be large. One rule of the thumb is not to use large feedback gain to avoid instability. The simulation demonstrates that MMC accepts both feedforward and feedback so that should one signal is lost, low frequency harmonics continue to be eliminated.

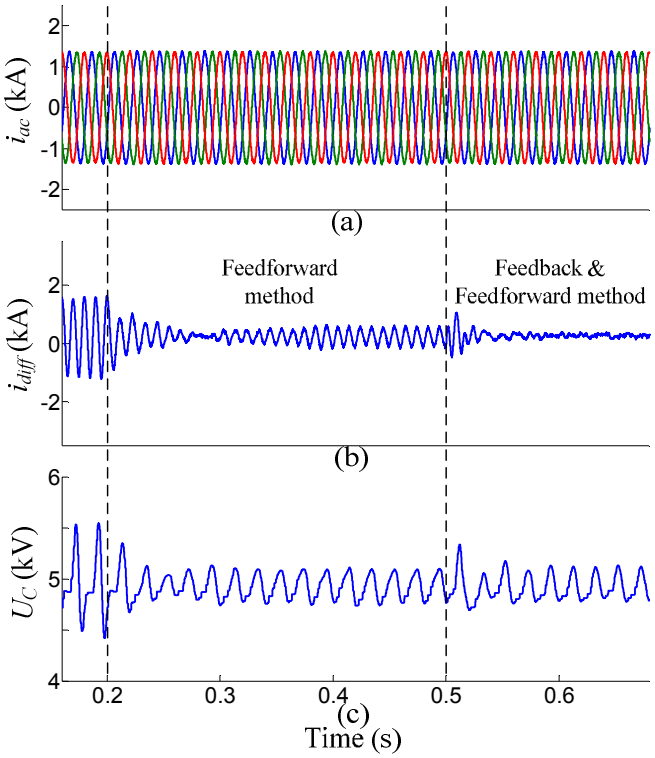


Fig. 11 2nd harmonic current elimination by feedback, then feedback-feedforward. (a) three phase MMC output currents; (b) $i_{diff}$; (c) capacitor voltage of one sub-module of phase A, upper arm.

*Test showing Deadbeat protecting 2nd Harmonic Feedforward- Feedback Elimination*

The graphs displayed in Fig. 12 are of the same variables as in Fig. 11. In addition to the feedback-feedforward 2nd Harmonic Elimination of Fig. 11, deadbeat reference change and 3-phase fault are activated. At t=0.6s, the current references of MMC step down to display the fast response of deadbeat shown in Fig. 12 (a). A 3-phase line-to-ground fault at PCC is simulated during $0.8s \leq t \leq 0.9s$. The simulation shows that deadbeat control keeps the ac current at values set by the current references as shown in Fig. 12 (a). Therefore in spite of the fault, circulating current $i_{diff}$ in Fig. 12 (b) and $U_C$ in Fig. 12 (c) are kept at safe values.

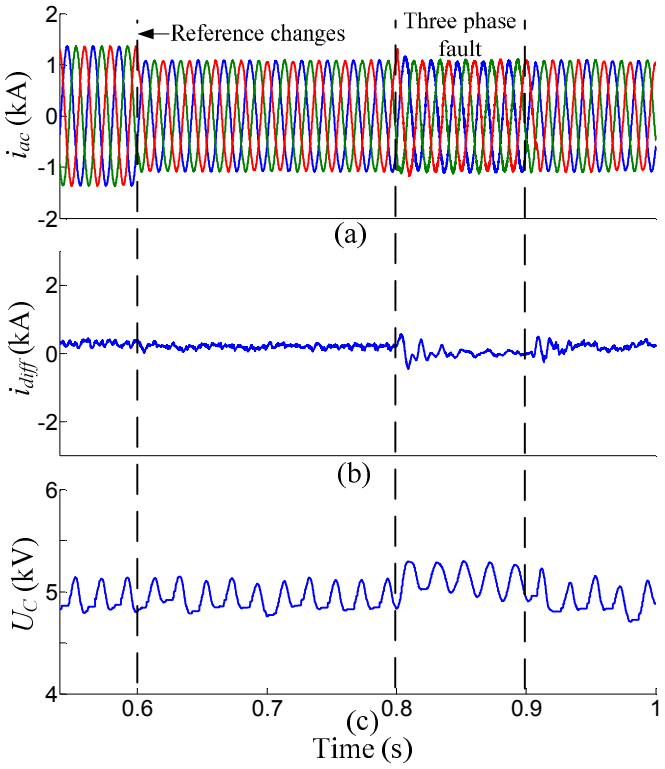


Fig. 12 Performance of the 2nd harmonic current elimination method when current reference changes at time 0.6s and under 3-phase line-to-ground fault condition (from time 0.8s~0.9s). (a) three phase MMC output currents; (b) $i_{diff}$; (c) capacitor voltage of one sub-module of phase A, upper arm.

## 7. Conclusion

This paper shows that MMC can simultaneously implement deadbeat and low frequency elimination by feedforward and feedback. With deadbeat, MMC becomes a reference current regulator; the ac currents in tracking the current references do not rise to destructively large values during ac faults. Likewise, inherent MMC harmonic currents on the ac-side cannot flow. This frees MMC from the necessity of having delta or open wye connected transformers—a measure taken to suppress the aforesaid MMC 3rd harmonics.

The paper shows that 2nd and low harmonics proliferated by the 2nd harmonic current can be eliminated by feedforward and feedback, singly or jointly. Deadbeat in preventing large fault currents to overcharge the capacitor voltages ensures the viability of the elimination methods.

The methods developed have multiple safeguards in harmonic elimination. Eliminating 2nd harmonics at the source by a combination of feedforward and feedback offers enhanced reliability. The elimination reduces the even harmonics on the dc-side and the 3rd and odd harmonics on the ac-side which are proliferated by the 2nd harmonic. In addition deadbeat suppresses harmonics on the ac side.

8. Acknowledgments

Mr. Can Wang thanks China Scholarship Council for financial support in pursuing the Ph.D. degree. Financial support by the Natural Science and Engineering Council (NSERC) of Canada through a Discovery Grant is acknowledged.

9. References

[1] S. Allebrod, R. Hamerski, and R. Marquardt, "New transformerless, scalable modular multilevel converters for HVDC-Transmission," in *Proc. Conf. Power Electron. Spec., Rhodes*, Greece, 2008, pp. 174–179.

[2] T. Westerweller, K. Friedrich, U. Armonies, A. Orini, D. Parquet, and S. When, "Trans bay cable—world's first HVDC system using multilevel voltage-sourced converter," in *Proc. CIGRE Conf. Power Syst.*, Paris, 2010, pp.1–6.

[3] M. Saeedifard and R. Iravani, "Dynamic performance of a modular multilevel back-to-back HVDC system," *IEEE Trans. Power Del.*, vol. 25, no. 4, pp. 2903–2912, Oct. 2010.

[4] J. Qin and M. Saeedifard, "Predictive Control of a Modular Multilevel Converter for a Back-to-Back HVDC System," *IEEE Trans. Power Del.*, vol. 27, no. 3, pp. 1538–1547, Jul. 2012

[5] E. Solas, G. Abad, J. Barrena, S. Aurtenetxea, A. Carcar, L. Zajac, "Modular Multilevel Converter With Different Submodule Concepts—Part II: Experimental Validation and Comparison for HVDC Application," *IEEE Trans. Ind. Electron.*, vol. 60, no. 10, pp. 4536–4545, Oct. 2013.

[6] R. Feldman, M. Tomasini, E. Amankwah, J.C. Clare, P.W. Wheeler, D.R. Trainer, R.S. Whitehouse, "A Hybrid Modular Multilevel Voltage Source Converter for HVDC Power Transmission," *IEEE Trans. Ind. Appl.*, vol. 49, no. 4, pp. 1577-1588, 2013.

[7] S. Kouro, M. Malinowski, K. Gopakumar, J. Pou, L.G. Franquelo, Bin Wu, J. Rodriguez, M.A. Perez, J.I. Leon, "Recent Advances and Industrial Applications of Multilevel Converters," *IEEE Trans. Ind. Electron.*, vol. 57, no. 8, pp. 2553–2580, Aug. 2010.

[8] M.A. Perez, R. Lizana F, J. Rodriguez, "Decoupled current control of modular multilevelconverter for HVDC applications," *IEEE Symposium on Industrial Electronics*, Hangzhou, China, 2012, pp. 1979-1984.

[9] M. Pereira, A. Zenkner, M.Claus, "Characteristics and benefits of modular multilevel converters for FACTS," *CIGRE 2010*, B4_104_2010.

[10] H.P. Mohammadi, M.T. Bina, "A Transformerless Medium-Voltage STATCOM Topology Based on Extended Modular Multilevel Converters," *IEEE Trans. Power Electron*., vol. 26, no. 5, pp. 1534-1545, 2011.

[11] J. Munoz, J. Espinoza, C. Baier, L. Moran, J. Guzman, V. Cardenas, "Decoupled and Modular Harmonic Compensation for Multilevel STATCOMs," *IEEE Trans. Ind. Electron.* (IEEE Early Access Articles).

[12] M. Hagiwara and H. Akagi, "Control and experiment of pulse-width-modulated modular multilevel converters," *IEEE Trans. Power Electron*., vol. 24, no. 7, pp. 1737–1746, Jul. 2009.

[13] M. Hagiwara, K. Nishimura, H. Akagi, "A Medium-Voltage Motor Drive With a Modular Multilevel PWM Inverter," *IEEE Trans. Power Electron*., vol. 25, no. 7, pp. 1786-1799, 2010.

[14] M. Hagiwara, R. Maeda, H. Akagi, "Control and Analysis of the Modular Multilevel Cascade Converter Based on Double-Star Chopper-Cells (MMCC-DSCC)," *IEEE Trans. Power Electron*., vol. 26, no. 6, pp. 1649-1658, 2011.

[15] J. Peralta, H. Saad, S. Dennetiere, J. Mahseredjian, S. Nguefeu, "Detailed and Averaged Models for a 401-Level MMC–HVDC System," *IEEE Trans. Power Del.*, vol. 27, no. 3, pp. 1501-1508, Jul. 2012.

[16] H. Saad, J. Peralta, S. Dennetiere, J. Mahseredjian, J. Jatskevich, J.A. Martinez, A. Davoudi, M. Saeedifard, V. Sood, X. Wang, J. Cano, A. Mehrizi-Sani, "Dynamic Averaged and Simplified Models for MMC-Based HVDC Transmission Systems," *IEEE Trans. Power Del.*, vol. 28, no. 3, pp. 1723-1730, Jul. 2013.

[17] N. Cherix, M. Vasiladiotis, A. Rufer, "Functional modeling and Energetic Macroscopic Representation of Modular Multilevel Converters," *Power Electronics and Motion Control Conference*, Novi Sad, Serbia, 2012, pp. 131-138.

[18] Antonopoulos, L. Angquist, and H. P. Nee, "On dynamics and voltage control of the modular multilevel converter," in *Proc. Eur. Conf. Power Electron. Appl.*, Barcelona, Spain, 2009, pp. 1–10.

[19] L. Harnefors, A. Antonopoulos, S. Norrga, L. Angquist, and H.-P. Nee, "Dynamic Analysis of Modular Multilevel Converters," *IEEE Trans. Ind. Electron.*, vol. 60, no. 7, pp. 2526-2537, Jul. 2013.

[20] K. Ilves, A. Antonopoulos, S. Norrga, and H.-P. Nee, "Steady-State Analysis of Interaction Between Harmonic Components of Arm and Line Quantities of Modular Multilevel Converters," *IEEE Trans. Power Electron.*, vol. 27, no. 1, pp. 57–68, 2012.

[21] L. Angquist, A. Antonopoulos, D. Siemaszko, K. Ilves, M. Vasiladiotis, and H.-P. Nee, "Open-Loop Control of Modular Multilevel Converters Using Estimation of Stored Energy," *IEEE Trans. Ind. Appl*., vol. 47, no. 6, pp. 2516-2524, 2011.

[22] Q. Song, W. Liu, X. Li, H. Rao, S. Xu, L. Li, "A Steady-State Analysis Method for a Modular Multilevel Converter," *IEEE Trans. Power Electron.*, vol. 28, no. 8, pp. 3702-3713, 2013.

[23] C. Wang, Q. Hao, B.T. Ooi, "Reduction of Low Frequency Harmonics in Modular Multilevel Converters (MMCs) by Harmonic Function Analysis," *IET Generation, Transmission & Distribution*, vol. 8, iss. 2, pp. 328-338, 2014

[24] Z. Li, P. Wang, H. Zhu, Z. Chu, Y. Li, "An Improved Pulse Width Modulation Method for Chopper-Cell-Based Modular Multilevel Converters," *IEEE Trans. Power Electron.*, vol. 27, no. 8, pp. 3472-3481, Aug. 2012.

[25] S. Rohner, S. Bernet, M. Hiller, R. Sommer, "Modulation, Losses, and Semiconductor Requirements of Modular Multilevel Converters," *IEEE Trans. Ind. Electron.*, vol. 57, no. 8, pp. 2633–2642, Aug. 2010.

[26] Y. Zhang, G.P. Adam, T.C. Lim, S.J. Finney, B.W. Williams, "Analysis of modular multilevel converter capacitor voltage balancing based on phase voltage redundant states," *IET Power Electron*., vol. 5, iss. 6, pp. 726-738, 2012.

[27] Q. Tu and Z. Xu, "Reduced Switching-Frequency Modulation and Circulating Current Suppression for Modular Multilevel Converters," *IEEE Trans. Power Del.*, vol. 26, no. 3, pp. 2009–2017, Jul. 2011.

[28] Q. Tu, Z. Xu, Y. Chang, L. Guan, "Suppressing DC Voltage Ripples of MMC-HVDC Under Unbalanced Grid Conditions," *IEEE Trans. Power Del.*, vol. 27, no. 3, pp. 1332–1338, Jul. 2012.

[29] Z. Li, P. Wang, Z. Chu, H. Zhu, Y. Luo, Y. Li, "An Inner Current Suppressing Method for Modular Multilevel Converters," *IEEE Trans. Power Electron.*, vol. 28, no. 11, pp. 4873-4879, Nov. 2013.

[30] G. Bergna, E. Berne, P. Egrot, P. Lefranc, A. Arzande, J.-C. Vannier, M. Molinas, "An Energy-Based Controller for HVDC Modular Multilevel Converter in Decoupled Double Synchronous Reference Frame for Voltage Oscillation Reduction," *IEEE Trans. Ind. Electron.*, vol. 60, no. 6, pp. 2360–2371, Jun. 2013.

[31] J. Moon, C. Kim, J. Park, D. Kang, J. Kim, "Circulating Current Control in MMC Under the Unbalanced Voltage," *IEEE Trans. Power Del.*, vol. 28, no. 3, pp. 1952–1959, Jul. 2013.

[32] Q. Hao, G. Li, B.T. Ooi, "Approximate model and low-order harmonic reduction for high-voltage direct current tap based on series single-phase modular multilevel converter," *IET Gener. Transm. Distrib*., vol. 7, iss. 9, pp. 1046-1054, 2013.

[33] S. Buso, L. Malesani, P. Mattavelli, "Comparison of Current Control Techniques for Active Filter Applications," *IEEE Trans. Power Electron.*, vol. 45, no.5. pp.722-729, 1998.

[34] A. Kawamura,P. Chuarayaratip, T. Haneyoshi,"'Deadbeat control of PWM inverter with modified pulse patterns for uninterruptible power supply," *IEEE Trans. Ind. Electron.*, vol. 35, no. 2, pp. 295-300, 1988.

[35] T. Kawabata, T. Miyashita,Y. Yamamoto, "Dead beat control of three phase PWM inverter," *IEEE Trans. Power Electron.*, vol. 5, no.1. pp.21-28, 1990.

[36] C. Hua,"Two-level switching pattern deadbeat DSP controlled PWM inverter," *IEEE Trans. Power Electron.*, vol. 10, no.3. pp.310-317, 1995.

[37] O.Kukrer, "'Deadbeat control of a three-phase inverter with an output LC-filter," *IEEE Trans. Power Electron.*, vol. 11, no.1. pp.16-23, 1996.

[38] O. Kukrer, H. Komurcugil, "Deadbeat control method for single-phase UPS inverters with compensation of computation delay," *IEE Proc.-Power Electronic Applications*, vol. 146, iss. 1, pp. 123-128, 1999.

[39] L.X. Tang and B. T. Ooi, "Elimination of Harmonic Transfer Through Converters in VSC-Based Multiterminal DC Systems by AC/DC Decoupling," *IEEE Trans. Power Del.*, vol. 23, no. 1, pp. 402-409, Jan. 2008.

[40] J.Hu, "Deatbeat Controlled PWM converter," M.Eng.Thesis, 1999, McGill University, Canada.

[41] X-M. Liu, Q. Zhang, Q. Zhao, Z-Q. Yao, "Research on Deadbeat control strategy of Modular Multilevel Converter", *International Conference on Transportation, Mechanical, and Electrical Engineering (TMEE)*, Changchun, China, 2011, pp. 621-624.

[42] A. Lesnicar and R. Marquardt, "An innovative modular multilevel converter topology suitable for a wide power range," in *Proc. Power Tech Conf.*, Bologna, Italy, 2003.

[43] E. Solas, G. Abad, J. Barrena, S. Aurtenetxea, A. Carcar, L. Zajac, "Modular Multilevel Converter With Different Submodule Concepts—Part I: Capacitor Voltage Balancing Method," *IEEE Trans. Ind. Electron.*, vol. 60, no. 10, pp. 4536–4545, Oct. 2013.

[44] B. Carter, Application Notes, Texas Instruments Incorporated. Application Report SLOA096, Dec. 2001.

## 10. Appendix

### 10.1 Appendix 1: Tables 1, 2, 3 and 4 from [23]

Table 1. AC-Side Equivalent Voltages

| | $\omega$ | $3\omega$ |
|---|---|---|
| $T_1$ | $\frac{NI_{ac}}{8\omega C}\sin(\omega t+\varphi_{ac})$ | --- |
| $T_4$ | $-\frac{NU_{ref}I_d}{2\omega CU_{dc}}\sin(\omega t+\delta)$<br>$-\frac{NU_{ref}X}{4\omega CU_{dc}}\sin(\omega t+\varphi_2-\delta)$ | $-\frac{NU_{ref}X}{12\omega CU_{dc}}\sin(3\omega t+\varphi_2+\delta)$ |
| $T_6$ | $-\frac{NU_{ref}}{CU_{dc}}\cos(\omega t+\delta)\cdot$<br>$\int_{-\infty}^{t}[\frac{I_d}{2}-\frac{U_{ref}I_{ac}}{4U_{DC}}\cos(\delta-\varphi_{ac})]d\tau$ | --- |
| $T_7$ | $-\frac{NU_{ref}X}{8\omega CU_{dc}}\sin(\omega t+\varphi_2-\delta)$<br>$\frac{NU_{ref}^2I_{ac}}{16\omega CU_{dc}^2}\sin(\omega t+\varphi_{ac})$ | $-\frac{NU_{ref}X}{8\omega CU_{dc}}\sin(3\omega t+\varphi_2+\delta)$<br>$\frac{NU_{ref}^2I_{ac}}{16\omega CU_{dc}^2}\sin(3\omega t+2\delta+\varphi_{ac})$ |

Table 2. DC-Side Equivalent Voltages

| | dc | $2\omega$ |
|---|---|---|
| $T_2$ | $\int_{-\infty}^{t}[\frac{I_d}{2}-\frac{U_{ref}I_{ac}}{4U_{DC}}\cos(\delta-\varphi_{ac})]d\tau$ | --- |
| $T_3$ | --- | $\frac{NX}{8\omega C}\sin(2\omega t+\varphi_2)$<br>$-\frac{NU_{ref}I_{ac}}{16\omega CU_{dc}}\sin(2\omega t+\delta+\varphi_{ac})$ |
| $T_5$ | $-\frac{NU_{ref}I_{ac}}{8\omega CU_{dc}}\sin(\varphi_{ac}-\delta)$ | $-\frac{NU_{ref}I_{ac}}{8\omega CU_{dc}}\sin(2\omega t+\delta+\varphi_{ac})$ |
| $T_8$ | $\frac{NU_{ref}^2X}{4\omega CU_{dc}^2}\sin(\varphi_2-2\delta)$ | $\frac{NU_{ref}^2I_d}{2\omega CU_{dc}^2}\sin(2\omega t+2\delta)$<br>$\frac{NU_{ref}^2X}{3\omega CU_{dc}^2}\sin(2\omega t+\varphi_2)$ |

Table 3. AC-Side Equivalent Voltages

| | $\omega$ | $3\omega$ |
|---|---|---|

| | | |
|---|---|---|
| $T_B$ | $\frac{NYI_{ac}}{8\omega CU_{dc}}\sin(\omega t+\gamma-\varphi_{ac})$ | $\frac{NYI_{ac}}{24\omega CU_{dc}}\sin(3\omega t+\gamma+\varphi_{ac})$ |
| $T_C$ | $-\frac{NU_{ref}YI_d}{4\omega CU_{dc}^2}\sin(\omega t+\gamma-\delta)$ | $-\frac{NU_{ref}YI_d}{4\omega CU_{dc}^2}\sin(3\omega t+\gamma+\delta)$ |
| $T_E$ | $-\frac{NYI_{ac}}{8\omega CU_{dc}}\sin(\omega t+\gamma-\varphi_{ac})$ | $\frac{NYI_{ac}}{8\omega CU_{dc}}\sin(3\omega t+\varphi_{ac}+\gamma)$ |
| $T_H$ | $\frac{NU_{ref}YI_d}{2\omega CU_{dc}^2}\sin(\omega t+\gamma-\delta)$ | $-\frac{NU_{ref}YI_d}{2\omega CU_{dc}^2}\sin(3\omega t+\gamma+\delta)$ |
| $T_J$ | $-\frac{NY^2I_{ac}}{12\omega CU_{dc}^2}\sin(\omega t+\varphi_{ac})$ | $\frac{NY^2I_{ac}}{8\omega CU_{dc}^2}\sin(3\omega t+2\varphi-\varphi_{ac})$ |

Table 4. DC-Side Equivalent Voltages

| | dc | $2\omega$ |
|---|---|---|
| $T_A$ | --- | $\frac{NYI_d}{4\omega CU_{dc}}\sin(2\omega t+\gamma)$ |
| $T_D$ | $-\frac{NU_{ref}YI_{ac}}{8\omega CU_{dc}^2}\sin(\gamma-\varphi_{ac}-\delta)$ | $-\frac{NU_{ref}YI_{ac}}{24\omega CU_{dc}^2}\sin(2\omega t+\gamma+\varphi_{ac}-\delta)$<br>$-\frac{NU_{ref}YI_{ac}}{8\omega CU_{dc}^2}\sin(2\omega t+\gamma-\varphi_{ac}+\delta)$ |
| $T_F$ | --- | $Y\cos(2\omega t+\gamma)$ |
| $T_G$ | $-\frac{NU_{ref}YI_{ac}}{16\omega CU_{dc}^2}\sin(\delta+\varphi_{ac}-\gamma)$ | --- |
| $T_I$ | --- | --- |

10.2 Appendix 2: Table 5 MMC Parameters

| Parameters | Values |
|---|---|
| Complex Power $P$ | 50 MW |
| Single station DC voltage $U_{dc}$ | 60 kV |

| | |
|---|---|
| Number of SM per arm N | 12 |
| SM capacitor voltage | 5 kV |
| Arm inductance $L_0$ | 3 mH |
| SM capacitance | 5000 μF |
| Equivalent transformer linkage inductance $L_T$ | 1 mH |
| AC voltage $U_{ac}$ | 30.6 kV |
| DC resistance $R_{dc}$ | 0.1 Ω |

GTD-2013-0944
Incorporating DEADBEAT and Low Frequency Harmonic Elimination in Modular Multilevel Converters (MMC) by Can Wang and Boon Teck Ooi

To Prof. Rehtanz
IET Generation, Transmission & Distribution
Editorial Office

Dear Sir:

Below are our responses to each of the reviewers' comments which are reproduced in italics. Our responses are in **bold** so as to stand out.

Reviewer: 1

Comments to the Author

*The paper is an insightful presentation for the incorporation of deadbeat in MMC. Actually, it is rather a state of the art on this very interesting technical aspect, with very good analysis as theoretically as in terms of simulation process. For these reasons it worths publication in IET GTD.*

**The authors are thankful for the encouragement.**

Reviewer: 2

Comments to the Author

*To the best of my limited knowledge of this specialized subject, the paper is a good description of an interesting piece of research work. It is clearly enough presented. However, it appears far too long for a journal paper, and should be considerably tightened.*

**The authors are thankful for the encouragement.**

**Regarding tightening, the authors would like to draw attention to the content coverage of subjects in the title: Incorporating DEADBEAT and Low Frequency Harmonic Elimination in Modular Multilevel Converters (MMC)**

**The main subjects are: 1. deadbeat, 2. Low Frequency Harmonic Elimination and 3. MMC. The table below presents an analysis based on Sections and the word count of each. In each section, there can be a few sub-sections.**

| Section | Title | Number of Words |
|---|---|---|
| | Abstract | 135 |
| 1 | Introduction | 526 |
| 2 | Modular Multilevel Converter (MMC) Topology and Control<br>MMC structure—used for simulation<br>Derivation of equations for Tables I, II, III and IV (relevant to understanding origin of harmonics and elimination by feedforward and feedback | 758 |
| 3 | Deadbeat Control<br>Open Loop<br>Closed Loop | 1175 |
| 4 | Simulation tests of MMC under deadbeat control | 373 |
| 5 | Feedforward and feedback harmonic elimination<br>Feedforward Method<br>Feedback Method | 376 |
| 6 | Simulation Tests on Harmonic Elimination and Deadbeat | 521 |
| 7 | Conclusions | 178 |

**There are many new concepts which require space to introduce and explain.**

**For example, our deadbeat is INDIVDUAL PHASE DEADBEAT which does not depend on balanced 3-phase where d-q transformation can be used. Thus our deadbeat is good for asymmetrical faults. The 1175 words include OPEN LOOP and CLOSED LOOP. To our regret, there is no space to describe CLOSED LOOP feedback adequately.**

**The origin of low frequency harmonics and their elimination by feed-forward are discovered by the authors. The authors also present their feedback method based on their innovative Complement Fliege Notch Filter.**

**Many words cannot be reduced: Sections 4 and 6 which present simulation results and References.**

**The authors are grateful that the reviewer thinks that the paper "is clearly enough presented." This is because the paper has been written several times to trim "fat" around so much "meat" in the text. However, they fear that after "butchering themselves", the clarity will be lost.**

Reviewer: 3

Comments to the Author

*This paper shows applications of deadbeat control to resolve some of the a.c. side current waveform problems. These problems are also being dealt with by other methods particularly those in rotating reference frames associated to the a.c. side grid voltage.*

**In the revision, the authors have written**
**"A distinctive feature of the deadbeat control in this paper is that it does not require d-q transformation. As an individual phase controller, it handles asymmetric operating conditions, such as a single-line fault."**

*The authors are suggested to compare their method with some of those methods, particularly in terms of transient response.*

**Experimental research by Dr. Mahdi Fazeli of the University of Malaya, Malaysia, confirms that Individual Phase Deadbeat has a delay of 2 time steps (see inset) as shown below. The result is from another author and cannot be used in this paper.**

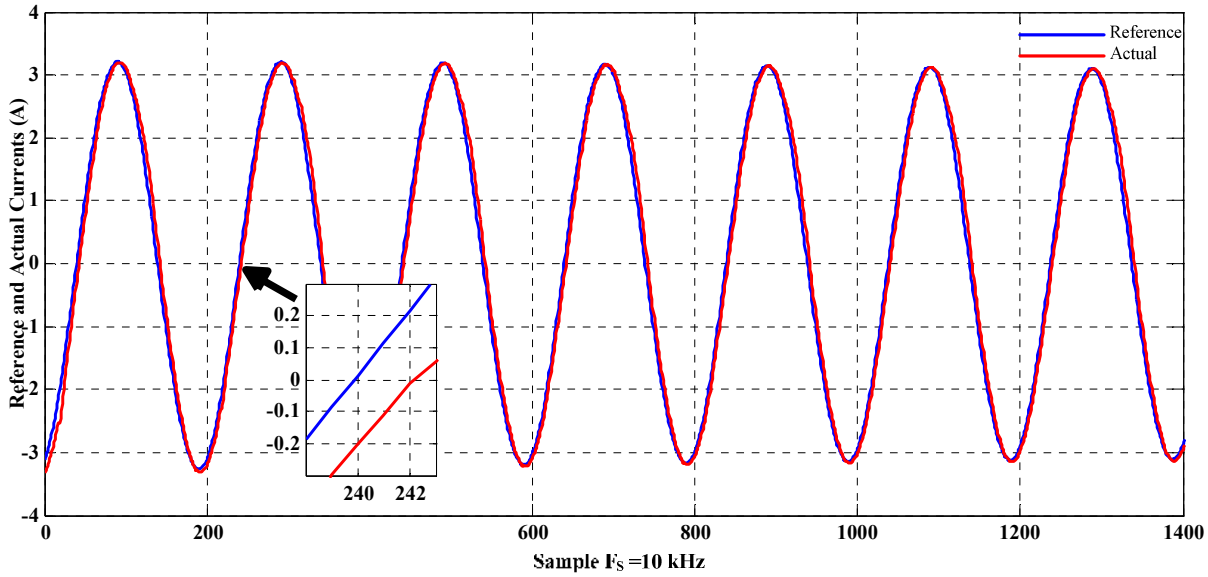


**Experiment result of Dead-beat Current control**

*Some specific comments are:*

*1. Figure 7(a). It is not clear how this was obtained. The physical reasons for such a high level of 3rd harmonic should be explained. Control with many other methods does not give such a high level of distortion.*

Control with many other methods does not give such a high level of distortion. This is because **"Normally, the ac sides of MMC stations are connected to transformers in delta or open wye to exclude the 3rd harmonic current generated by T4."**

**The reason for a high level of distortion is because the simulation test consists of connecting the MMC to transformers in wye with the neutral grounded. As shown in Fig. 7 (a), the 3-phase current waveforms have large 3rd harmonics, confirming the predictions of [23].**

**The explanation is complete in the original text below the caption of Fig. 7, because the original text reads:**

**'T4 in Table I of [23] has a 3rd harmonic voltage component on the ac-side. Normally, the ac sides of MMC stations are connected to transformers in delta or open wye to exclude the 3rd harmonic current generated by T4. The simulation test consists of connecting the MMC to transformers in wye with the neutral grounded. As shown in Fig. 7 (a), the 3-phase current waveforms have large 3rd harmonics, confirming the predictions of [23].'**

*2. Throughout the paper, it is not clear how the reference values (waveforms) of the a.c. side currents are to be obtained in practice – during normal or fault conditions. If these are to be obtained in a d-q reference frame, what would be the advantage of deadbeat control?*

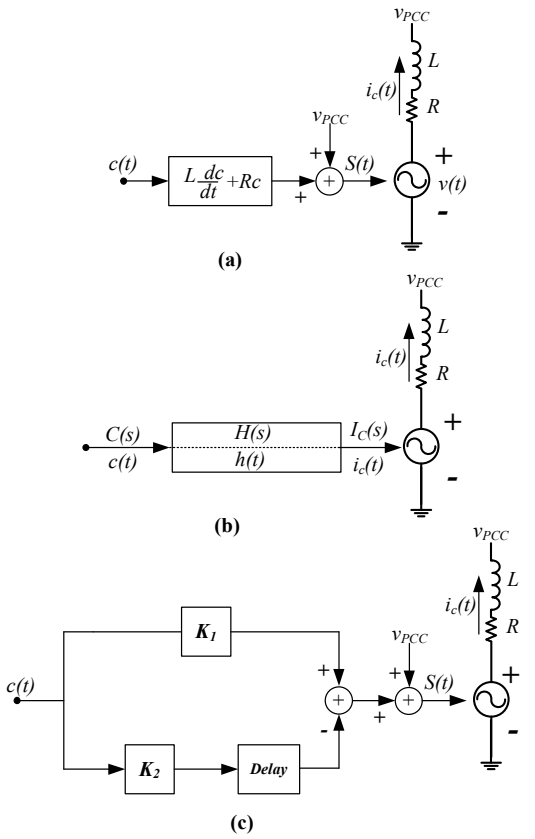


**The reference current control of the INDIVIDUAL PHASE Deadbeat is c(t) in Fig. (c). The MMC outputs voltage T6 which from (18)**

**is**

$$T_6 = -\frac{NU_{ref}}{CU_{dc}}\cos(\omega t+\delta)\cdot\int_{-\infty}^{t}[\frac{I_d}{2}-\frac{U_{ref}I_{ac}}{4U_{DC}}\cos(\delta-\varphi_{ac})]d\tau$$
$$= -\frac{U_{ref}}{U_{dc}}\cos(\omega t+\delta).2T_2 = -U_{ref}\cos(\omega t+\delta) \quad \textbf{(18)}$$

**$S(t) = U_{ref}\cos(\omega+\delta)/U_{dc}$ is the voltage reference signal in the modulating signals of MMC**

$$m_U(t) = \frac{1}{2}-\frac{U_{ref}}{U_{dc}}\cos(\omega t+\delta) \quad \textbf{(1-a)} \qquad m_L(t) = [\frac{1}{2}+\frac{U_{ref}}{U_{dc}}\cos(\omega t+\delta)] \quad \textbf{(1-b)}$$

**In reference current control, the current reference signal c(t), after passing through the "deadbeat black box", is added to the voltage at the Point of Common Coupling $v_{PCC}(t)$ to become S(t).**

**During a single-phase line to ground fault, the voltage at the terminal of that phase becomes $v_{PCC}(t) \rightarrow 0$ for that phase alone. As a result, S(t) produces a voltage large enough to force through R and L to produce the current required by the reference c(t).**

**Each phase has its Fig. (c). The current references are: $c_a(t)$, $c_b(t)$ $_c$c(t). Each phase has its feedforward voltages $v_{PCC-a}(t)$, $v_{PCC-b}(t)$, $v_{PCC-c}(t)$. There is no reason for having d-q transformation.**

**The long explanation using Fig. (a), fig (b) and Fig(c) should have already conveyed the ideas. For this reason, there is little "fat" to be trimmed to tighten the paper.**

3. *The open-loop deadbeat control is dependent on the knowledge of system parameters.*

**The text in Section 3-B has the following highlighted text added:**

**MMC has to operate in the face of uncertainties. The voltages $v_{PCC-a}(t)$, $v_{PCC-b}(t)$ and $v_{PCC-c}(t)$ at the points of common coupling immunize, to some extent, the uncertainties in the ac-circuits outside the MMC. Because the components L and R belong to the manufacturer and can be measured precisely, deadbeat can be designed with confidence.**

This dependency is reduced in closed-loop control.

**But parameters change with temperature and other climatic factors. Close loop feedback control, in general, makes performance insensitive to parameter variations. Closed loop feedback control is implemented as shown in Fig. 6 [40].**

But how does this compare to other closed loop control methods?

**In [40], close loop feedback immunizing deadbeat against small parameter changes in R and L has been demonstrated by simulations. But this information is not in the paper.**